THE MULTIVARIABLE STRUCTURE FUNCTION AS AN EXTENSION OF THE RGA MATRIX: RELATIONSHIP AND ADVANTAGES

Luis A. Amézquita-Brooks
CIIIA-FIME
UANL
México
luis.amezquita@uanl.mx

Carlos E. Ugalde-Loo
Institute of Energy
Cardiff University
Wales, UK
Ugalde-LooC@cardiff.ac.uk

Eduardo Licéaga-Castro
CIIIA-FIME
UANL
México
e.liceaga.c@gmail.com

Jesús Licéaga-Castro
Depto. de Electrónica
UAM-Azcapotzalco
México
ucastro21@hotmail.com

Abstract

It is common practice to specify the performance of control design tasks in terms of an output response to a given input. In spite of a greater complexity, this is also the case for multivariable plants, where for clarity of performance specification and design remains desirable to consider the inputs and outputs in pairs. Regardless of the structure and internal coupling of the plant, it is convenient to establish if decentralized control is capable of meeting design specifications: the control structure will be easy to implement, economic (less programming burden upon implementation), and may provide further physical insight. In line with this, the analysis and design of decentralized controllers using the relative gain array (RGA) and the multivariable structure function (MSF) are presented for the general multivariable case. It is demonstrated that the RGA matrix can be expressed in terms of the MSF. Moreover, it is shown that the correct interpretation of the MSF offers significative advantages over the RGA matrix analysis. While the RGA offers insight about the adequate pairing of input-output signals in a multivariable system, the MSF, besides providing this information, plays a crucial role in the design of stabilizing controllers (and their requirements) and the subsequent robustness and performance assessment of the closed loop control system. Theoretical results are drawn for a general $n \times n$ plant, with examples from electrical power systems and laboratory tank processes included to illustrate key concepts.

1 The Relative Gain Array Matrix

The relative gain array (RGA) matrix, proposed by [Bristol, 1966], is defined as:

$$\mathbf{\Lambda}\big(\mathbf{G}(s)\big) = \mathbf{G}(s) \times \big(\mathbf{G}(s)^{-1}\big)^T, \qquad (1)$$

where $\times$ denotes an element-by-element multiplication and $\mathbf{G}(s)$ is an $n \times n$ square transfer matrix:

$$\mathbf{G}(s) = \begin{bmatrix} g_{11}(s) & g_{12}(s) & \dots & g_{1n}(s) \\ g_{21}(s) & g_{22}(s) & \dots & g_{2n}(s) \\ \vdots & \vdots & \ddots & \vdots \\ g_{n1}(s) & g_{n2}(s) & \dots & g_{nn}(s) \end{bmatrix}. \qquad (2)$$

Historically, the use of the RGA matrix has been focused on decentralized (diagonal) control. In particular, the following rules regarding the pairing of input-output control channels are employed [Skogestad and Postlethwaite, 2005]:

i. An input-output pairing such that the diagonal elements of the RGA matrix are close to one is preferable since this pairing is related with a diagonal dominant plant.

ii. Avoid input-output pairings which generate diagonal negative elements on the RGA matrix with

$s = 0$. This condition is closely related to systems with lack of integrity; *i.e.*, a system which cannot maintain stability if one of the diagonal closed loops is open.

iii. High positive values in the diagonal elements of the RGA matrix indicate difficulty for designing diagonal controllers.

The RGA matrix has proved to be a valuable tool in the selection of input-output pairing for diagonal control design. In general RGA can be interpreted in the frequency domain, but it is commonly used to evaluate the coupling of input-output pairings at steady state [Bristol, 1966; Grosdidier, Morari and Holt, 1985]. However, it has been observed that rule i should be applied with $s = j\omega_{BW}$, where ω_{BW} is the crossover frequency of the open loop system [Mc Avoy, Arkun, Chen, Robinson and Schnelle, 2003; Skogestad and Postlethwaite, 2005].

Even when the use of the RGA matrix is widely accepted, developments of the key aspects which are contained within the theoretical foundations of the RGA matrix have not been fully analyzed. The main idea around the RGA matrix is to assess the effect a controller of each output variable would have on a specific open loop variable. In fact, the *ij*-th element of matrix $\mathbf{\Lambda}\big(\mathbf{G}(s)\big)$ may be defined as follows:

$$\lambda_{ij} = \frac{g_{ij}(s)}{\hat{g}_{ij}(s)}, \tag{3}$$

where $\hat{g}_{ij}(s)$ is the resulting open loop response between the j-th input and the i-th output with all the remaining outputs set under the influence of a diagonal controller of appropriate dimensions.

It would seem logical to ask what would be the stability and robustness characteristics of such a controller. Some effort in this direction was presented in [Grosdidier, Morari and Holt, 1985; Chiu and Arkun, 1990; Skogestad and Postlethwaite, 2005], where the integrity of the control system in relation with the RGA matrix was investigated. However, the RGA matrix does not play any role in the design stage of the controller. Moreover, its use has been restricted to those systems which can be made diagonal dominant by the simple commutation of input-output pairings.

In a completely independent fashion, a multivariable design framework called individual channel analysis and design (ICAD), which deals with the design of diagonal controllers for multivariable plants, was proposed in the early 90s [O'Reilly and Leithead, 1991]. Although not widespread, this framework proved useful in solving difficult control problems associated to non-diagonally dominant, unstable, non-minimum phase and non-square plants [Licéaga-Castro, Licéaga-Castro and Ugalde-Loo, 2005; Licéaga-Castro, Licéaga-Castro and Amézquita-Brooks, 2005; Licéaga-Castro, Ramírez-España and Licéaga-Castro, 2006; Licéaga-Castro, Licéaga-Castro, Ugalde-Loo and Navarro-López, 2008;

Licéaga-Castro, Amézquita-Brooks and Licéaga-Castro, 2008; Licéaga-Castro, Navarro-López and Licéaga-Castro, 2008; Ugalde-Loo, 2009].

ICAD allows the use of classical SISO robustness margins (phase and gain margins) for MIMO control systems. The key component of the ICAD framework is the *multivariable structure function* (MSF) which illuminates several important issues of the open loop system. In particular, it allows

- elucidating the minimum phase conditions of the transmission zeros;
- measuring the cross-coupling between input-output pairs;
- using the Nyquist stability criterion, and all its associated robustness margins, for measuring the possibility of direct decoupling of the system.

It is clear that a close relationship between the MSF and the RGA matrix should exist since through both tools appropriate input-output pairings can be defined. In the next sections this relation will be fully revealed and some common features will be analyzed. However, it should be noticed that the most important features of the MSF are not related with the analysis of the open loop system. As a matter of fact, the MSF plays a crucial part both in the controller design process and in the subsequent robustness assessment of the closed loop control system.

2 The Multivariable Structure Function

Consider an $n \times n$ system $\mathbf{G}(s)$ with a diagonal controller matrix $\mathbf{K}(s)$:

$$\begin{aligned} \mathbf{Y}(s) &= \mathbf{G}(s)\mathbf{U}(s), \\ \mathbf{U}(s) &= \mathbf{K}(s)\mathbf{E}(s), \\ \mathbf{E}(s) &= \mathbf{R}(s) - \mathbf{Y}(s), \end{aligned} \tag{4}$$

where $\mathbf{R}(s)$ is a reference vector. The output and input signal vectors are defined, respectively, as follows:

$$\begin{aligned} \mathbf{Y}(s) &= \begin{bmatrix} y_1(s) \ y_2(s) \ \dots \ y_n(s) \end{bmatrix}^T, \\ \mathbf{U}(s) &= \begin{bmatrix} u_1(s) \ u_2(s) \ \dots \ u_n(s) \end{bmatrix}^T. \end{aligned}$$

The closed loop dynamics of (4) are given by:

$$\begin{aligned} \mathbf{Y}(s) &= \mathbf{G}(s)\mathbf{K}(s)\big(\mathbf{I} + \mathbf{G}(s)\mathbf{K}(s)\big)^{-1}\mathbf{R}(s) \\ &= \mathbf{H}(s)\mathbf{R}(s). \end{aligned} \tag{5}$$

The individual channel concept is set up to investigate the cross-coupling of a particular group of input-output variables against the remaining variables. That is, system $\mathbf{G}(s)$ may be partitioned as

$$\mathbf{G}(s) = \left[\begin{array}{c|c} \mathbf{G}_{11}(s) & \mathbf{G}_{12}(s) \\ \hline \mathbf{G}_{21}(s) & \mathbf{G}_{22}(s) \end{array} \right], \tag{6}$$

with

$$\mathbf{Y}(s) = \left[\begin{array}{c} \mathbf{Y}_1(s) \\ \hline \mathbf{Y}_2(s) \end{array} \right], \ \mathbf{K}(s) = \left[\begin{array}{c|c} \mathbf{K}_{11}(s) & \mathbf{0} \\ \hline \mathbf{0} & \mathbf{K}_{22}(s) \end{array} \right],$$
$$\mathbf{R}(s) = \left[\begin{array}{c} \mathbf{R}_1(s) \\ \hline \mathbf{R}_2(s) \end{array} \right], \quad \mathbf{E}(s) = \left[\begin{array}{c} \mathbf{E}_1(s) \\ \hline \mathbf{E}_2(s) \end{array} \right]. \tag{7}$$

A block diagram depicting the system described by (6) and (7) is shown in Figure 1.
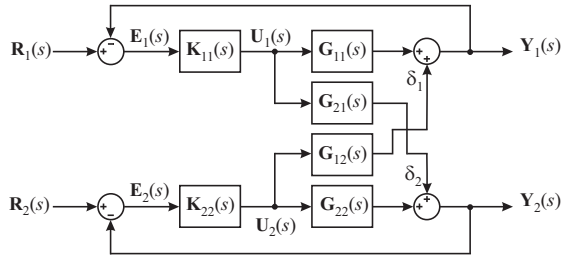

Figure 1.   Block diagram representation of a partitioned multivariable control system with a diagonal controller.
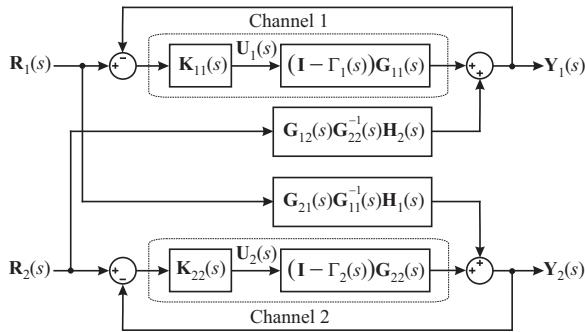

Figure 2.   Equivalent control system using individual channel representation.

For the following procedure the Laplace operator is dropped for convenience. According to Figure 1,

$$\mathbf{Y}_1 = \mathbf{G}_{11}\mathbf{U}_1 + \mathbf{G}_{12}\mathbf{U}_2.$$

Notice that $\mathbf{U}_2(s)$ may also be written as

$$\mathbf{U}_2 = \mathbf{X}_2\boldsymbol{\delta}_2,$$

where

$$\boldsymbol{\delta}_2 = \mathbf{G}_{21}\mathbf{U}_1.$$

$\mathbf{X}_2(s)$ can be easily obtained noting that

$$\mathbf{U}_2 = \mathbf{K}_{22}\mathbf{E}_2,$$
$$\mathbf{E}_2 = \mathbf{R}_2 - (\mathbf{G}_{22}\mathbf{U}_2 + \boldsymbol{\delta}_2).$$

By using the superposition theorem and considering $\mathbf{R}_2(s) = \mathbf{0}$, then

$$\mathbf{U}_2 = -\mathbf{K}_{22}(\boldsymbol{\delta}_2 + \mathbf{G}_{22}\mathbf{U}_2).$$

A rearrangement of the previous expression by using the "push through" rule [Helton, Stankus and Wavrik, 1998] yields

$$\mathbf{U}_2 = -\mathbf{K}_{22}(\mathbf{I} + \mathbf{G}_{22}\mathbf{K}_{22})^{-1}\boldsymbol{\delta}_2.$$

Considering this, $\mathbf{Y}_1(s)$ can be rewritten as

$$\mathbf{Y}_{1a} = \mathbf{G}_{11}\mathbf{U}_1 - \mathbf{G}_{12}\mathbf{K}_{22}(\mathbf{I} + \mathbf{G}_{22}\mathbf{K}_{22})^{-1}\mathbf{G}_{21}\mathbf{U}_1,$$

where $\mathbf{Y}_{1a}(s)$ was introduced to remark that $\mathbf{R}_2(s) = \mathbf{0}$. Since the closed loop of the diagonal open loop transfer matrix $\mathbf{G}_{22}(s)\mathbf{K}_{22}(s)$ can be expressed as

$$\mathbf{H}_2 = \mathbf{G}_{22}\mathbf{K}_{22}(\mathbf{I} + \mathbf{G}_{22}\mathbf{K}_{22})^{-1},$$

it is clear then that

$$\mathbf{Y}_{1a} = \left(\mathbf{I} - \mathbf{G}_{12}\mathbf{G}_{22}^{-1}\mathbf{H}_2\mathbf{G}_{21}\mathbf{G}_{11}^{-1}\right)\mathbf{G}_{11}\mathbf{K}_{11}\mathbf{E}_1,$$

or, more compactly,

$$\mathbf{Y}_{1a} = (\mathbf{I} - \boldsymbol{\Gamma}_1)\mathbf{G}_{11}\mathbf{K}_{11}\mathbf{E}_1 = \mathbf{C}_1\mathbf{E}_1, \qquad (8)$$

where

$$\mathbf{C}_1(s) = (\mathbf{I} - \boldsymbol{\Gamma}_1(s))\mathbf{G}_{11}(s)\mathbf{K}_{11}(s) \qquad (9)$$

represents Individual Channel 1 and models the open loop response of the output variables $\mathbf{Y}_1(s)$ under the fact that variables $\mathbf{Y}_2(s)$ operate in closed loop with controller $\mathbf{K}_2(s)$. The key element of the preceding analysis is the presence of MSF $\boldsymbol{\Gamma}_1(s)$, defined as

$$\boldsymbol{\Gamma}_1 = \mathbf{G}_{12}(s)\mathbf{G}_{22}(s)^{-1}\mathbf{H}_2(s)\mathbf{G}_{21}(s)\mathbf{G}_{11}(s)^{-1}, \quad (10)$$

which will be shown in Section 3 to be closely related to the RGA matrix.

In order to expose the effect of $\mathbf{R}_2(s)$ over $\mathbf{Y}_1(s)$, consider that the control loop over $\mathbf{E}_1(s)$ is open. This implies that

$$\mathbf{E}_2(s) = \mathbf{R}_2(s) - \mathbf{Y}_2(s).$$

Thus,

$$\begin{aligned}\mathbf{U}_2(s) &= \mathbf{K}_{22}(s)\left(\mathbf{I} + \mathbf{G}_{22}(s)\mathbf{K}_{22}(s)\right)^{-1}\mathbf{R}_2(s), \\ &= \mathbf{G}_{22}(s)^{-1}\mathbf{H}_2(s)\mathbf{R}_2(s).\end{aligned}$$

This rearrangement is represented in the block diagram of Figure 2, where the corresponding equations for Individual Channel 2 can be derived by simple symmetry. In particular:

$$\boldsymbol{\Gamma}_2(s) = \mathbf{G}_{21}(s)\mathbf{G}_{11}(s)^{-1}\mathbf{H}_1(s)\mathbf{G}_{12}(s)\mathbf{G}_{22}(s)^{-1},$$
$$\mathbf{H}_1(s) = \mathbf{G}_{11}(s)\mathbf{K}_{11}(s)\left(\mathbf{I} + \mathbf{G}_{11}(s)\mathbf{K}_{11}(s)\right)^{-1}.$$

The importance of MSFs $\boldsymbol{\Gamma}_i(s)$ becomes clear when, for instance, $\boldsymbol{\Gamma}_1(s) = \mathbf{0}$. This situation implies that the open loop response of variables $\mathbf{Y}_1(s)$ are equal to $\mathbf{G}_{11}(s)\mathbf{K}_{11}(s)\mathbf{E}_1(s)$ if $\mathbf{R}_2(s) = \mathbf{0}$. That is, subsystem $\mathbf{G}_{11}(s)$ is not coupled with subsystem $\mathbf{G}_{22}(s)$ through controller $\mathbf{K}_{11}(s)$. This indicates that it is possible to design $\mathbf{K}_{11}(s)$ on the basis of $\mathbf{G}_{11}(s)$ only.

The assumption that $\mathbf{R}_2(s) = \mathbf{0}$ can be lifted with no real consequences provided that the closed loop sensitivity of $\mathbf{G}_{11}(s)\mathbf{K}_{11}(s)$ is able to reject the perturbation $\mathbf{G}_{12}(s)\mathbf{G}_{22}(s)^{-1}\mathbf{H}_2(s)\mathbf{R}_2(s)$. Even if that is not

the case, the stability of the system is not compromised given that $\mathbf{H}_2(s)$ is stable. Therefore, the MSFs $\mathbf{\Gamma}_i(s)$ effectively measure the coupling of the system. A high value of $||\mathbf{\Gamma}_i(j\omega_0)||$ (using an appropriate norm) indicates a high coupling between variables $\mathbf{Y}_1(s)$ and $\mathbf{Y}_2(s)$ at frequency ω_0. Such a notion of coupling allows the introduction of a clear measurement of cross-coupling.

A full treatment of the ICAD framework is out of the scope of this article. However, it will be shown that the MSF contains all the information provided by the RGA matrix and much more.

3 Relation Between the RGA Matrix and the MSF

The contexts in which the RGA matrix and the MSF were derived are different: while the RGA matrix was obtained for open loop plant analysis [Bristol, 1966], the MSF was established as a means to measure the robustness of the closed loop system in the context of control system design [O'Reilly and Leithead, 1991]. Nonetheless, equivalent assumptions may be considered for both.

For instance, when calculating λ_{ij}, the ij-th element of the RGA matrix $\mathbf{\Lambda}\big(\mathbf{G}(s)\big)$ defined in (3), it is assumed that all outputs, excluding y_i, are perfectly controlled using all inputs, excluding u_j. In this context the open loop response of the free input-output variables y_i and u_j is denoted as $\hat{g}_{ij}(s)$. Such perfect control assumption can be also made within the ICAD framework. In this case, it is assumed that variables $\mathbf{Y}_2(s)$ are perfectly controlled via inputs $\mathbf{U}_2(s)$, which is equivalent to assuming $\mathbf{Y}_2(s) = \mathbf{R}_2(s)$. In this situation the input-output response between references $\mathbf{R}_2(s)$ and outputs $\mathbf{Y}_2(s)$ is given by $\mathbf{Y}_2(s) = \mathbf{H}_2(s)\mathbf{R}_2(s)$, since the variables $\mathbf{Y}_1(s)$ and inputs $\mathbf{U}_1(s)$ are operating in open loop (see Figure 1). Therefore, $\mathbf{Y}_2(s) = \mathbf{R}_2(s)$ is equivalent to $\mathbf{H}_2(s) = \mathbf{I}$.

Nevertheless, whilst the MSF and the individual channel definitions allow for multivariable individual channels, or multi-channels [Leithead and O'Reilly, 1992], the RGA matrix elements λ_{ij} consider only scalar "free" input-output variables. Employing such a consideration with scalar input u_1 and output y_1, for instance, is equivalent to assume that $\mathbf{Y}_1(s) = y_1(s)$ and $\mathbf{U}_1(s) = u_1(s)$. Under these conditions and since $\mathbf{U}_1(s) = \mathbf{K}_{11}(s)\mathbf{E}_1(s)$, it is easy to show from (8) that

$$y_1(s) = \big(1 - \gamma_1(s)\big)g_{11}(s)u_1(s),$$

where

$$\gamma_1(s) = \mathbf{G}_{12}(s)\mathbf{G}_{22}(s)^{-1}\mathbf{G}_{21}(s)g_{11}(s)^{-1}$$

is the scalar MSF which relates Individual Channel 1 and the multi-channel formed by all the remaining outputs. The relationship between λ_{11} and $\gamma_1(s)$ is finally revealed by noting that

$$\hat{g}_{11}(s) = \big(1 - \gamma_1(s)\big)g_{11}(s).$$

Thus,

$$\lambda_{11} = \frac{g_{11}(s)}{\hat{g}_{11}(s)} = \frac{1}{\big(1 - \gamma_1(s)\big)}. \tag{11}$$

The previous analysis may be generalized for the remaining elements of the RGA matrix by simple symmetry. In general, the ij-th element of the RGA matrix may be written as

$$\lambda_{ij} = \frac{1}{\big(1 - \gamma_{ij}(s)\big)}, \tag{12}$$

where $\gamma_{ij}(s)$ is the MSF which relates the i-th output with the j-th input assuming that all remaining outputs are controlled perfectly with the remaining inputs. MSF $\gamma_{ij}(s)$ can be obtained by rearranging the columns (or rows) of transfer matrix $\mathbf{G}(s)$ into $\hat{\mathbf{G}}(s)$ so that the i-th output and the j-th input of $\mathbf{G}(s)$ become the first output and the first input of $\hat{\mathbf{G}}(s)$. This way,

$$\gamma_{ij}(s) = \hat{\mathbf{G}}_{12}(s)\hat{\mathbf{G}}_{22}(s)^{-1}\hat{\mathbf{G}}_{21}(s)\hat{g}_{11}(s)^{-1},$$

which is obtained by rearranging the inputs and output pairs of a diagonal controller.

For instance, consider a simple 2×2 control system; i.e., $\mathbf{G}_{ij}(s) = g_{ij}(s)$, with $i, j = 1, 2$. In this case,

$$\gamma_{11}(s) = \frac{g_{12}(s)g_{21}(s)}{g_{11}(s)g_{22}(s)}. \tag{13}$$

It is known that for a 2×2 system [Skogestad and Postlethwaite, 2005],

$$\lambda_{11} = \frac{1}{\left(1 - \dfrac{g_{12}(s)g_{21}(s)}{g_{11}(s)g_{22}(s)}\right)}. \tag{14}$$

For systems of higher order [Grosdidier, Morari and Holt, 1985; Skogestad and Postlethwaite, 2005],

$$\lambda_{ii} = \frac{g_{ii}(s)\det\mathbf{G}^{ii}}{\det\mathbf{G}(s)}, \tag{15}$$

where $\mathbf{G}^{ii}$ is the minor of the ii-th element of $\mathbf{G}(s)$. Therefore, it follows from (12) and (15) that

$$\gamma_{ii}(s) = \frac{\lambda_{ii} - 1}{\lambda_{ii}} = 1 - \frac{\det\mathbf{G}(s)}{g_{ii}(s)\det\mathbf{G}^{ii}}. \tag{16}$$

The off-diagonal elements of the RGA matrix $\mathbf{\Lambda}\big(\mathbf{G}(s)\big)$ can be related with the MSF by swapping the appropriate rows (or columns) in $\mathbf{G}(s)$.

The previous result sheds light on the nature of the MSF. The individual channels considering the perfect control condition and a scalar output for $y_1(s)$ may be written as

$$c_i(s) = k_{ii}(s)g_{ii}(s)\big(1 - \gamma_i(s)\big). \tag{17}$$

Then, considering (16) and $\mathbf{H}_i(s) = \mathbf{I}$ yields:

$$c_i(s) = k_{ii}(s) \cdot \frac{\det \mathbf{G}(s)}{\det \mathbf{G}^{ii}}. \qquad (18)$$

Equation (18) reveals the relationship between the MSF and the RGA matrix within the ICAD context. However, it is important to emphasize that whereas the RGA matrix is only used to define input-output pairs selection as a previous step to diagonal control design, the MSF goes far beyond the input-output channels definition: it is fundamental to the control design, it defines the existence of stabilizing controllers, it sets the framework to establish the system robustness, and it permits the use of the phase and gain margin concepts in a rather effective manner.

4   Differences Between the RGA and the MSF

The main differences between the RGA matrix and the MSF are summarized as follows:

- The inclusion of the controller effects in the MSF allows its use as a measure of closed loop robustness.
- The RGA and the MSF have an interpretation in the frequency domain. However, the MSF analysis (magnitude and phase) is crucial to determine the existence of stabilizing controllers and their requirements [O'Reilly and Leithead, 1991].
- The MSF is not necessarily a scalar function. This allows using the MSF to measure the cross-coupling between arbitrary groups of output-input pairings. This is of great significance in processes where it is not possible to find decoupled scalar input-output pairs, but where decoupled groups of such pairings exist. For instance, in airplanes the variables relating the longitudinal and horizontal dynamics are both highly coupled systems which, nonetheless are considered as decoupled among them [Cook, 2012].

5   Illustrative Example 1: Power Systems

In order to illustrate the results presented in Section 3 and to address the points from Section 4, consider the system described in Figure 3. It corresponds to a synchronous generator feeding into a large system (represented by an infinite bus) via a tie-line system including a shunt compensator in the form of a Static VAr Compensator (SVC). The main application of an SVC is to provide dynamic reactive power support to enable effective voltage regulation and to enhance transient stability [Aree and Acha, 1999]. However, if a damping control loop is included, the device is also capable to provide damping for electromechanical oscillations [Mithulananthan, Canizares, Reeve and Rogers, 2003]. Figure 4 shows a block diagram of the system.

The synchronous machine – SVC system can be represented as the 3×3 system shown in Figure 4 [Ugalde-Loo, Acha and Licéaga-Castro, 2010]. The transfer matrix representation of such a system has the form

$$\begin{bmatrix} \Delta\omega(s) \\ \Delta e_t(s) \\ \Delta V_{SVC}(s) \end{bmatrix} = \begin{bmatrix} g_{11}(s) & g_{12}(s) & g_{13}(s) \\ g_{21}(s) & g_{22}(s) & g_{23}(s) \\ g_{31}(s) & g_{32}(s) & g_{33}(s) \end{bmatrix} \begin{bmatrix} \Delta P_m(s) \\ \Delta E_{fd}(s) \\ \Delta\alpha(s) \end{bmatrix}$$
$$(19)$$

or, more compactly,

$$\mathbf{Y}_{SVC}(s) = \mathbf{G}_{SVC}(s)\mathbf{U}_{SVC}(s), \qquad (20)$$

where $\mathbf{G}_{SVC}(s)$ is the transfer matrix. The individual elements of $\mathbf{G}_{SVC}(s)$ can be explicitly found in [Ugalde-Loo, Acha, Licéaga-Castro and Licéaga-Castro, 2008]. The synchronous machine parameters and operating condition are provided in [Ugalde-Loo, Acha and Licéaga-Castro, 2010].
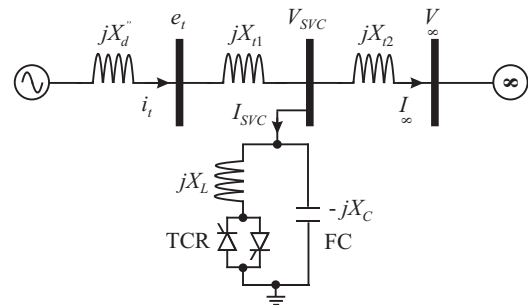

Figure 3. Synchronous generator – SVC system [Ugalde-Loo, Acha and Licéaga-Castro, 2010].
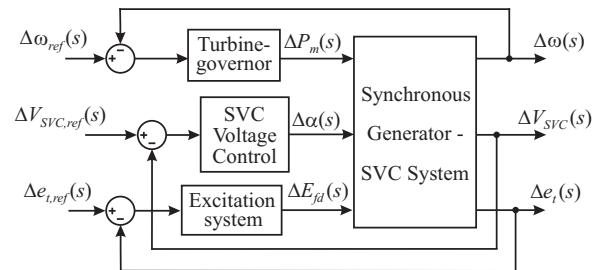

Figure 4. Block diagram of the synchronous generator – SVC system [Ugalde-Loo, Acha and Licéaga-Castro, 2010].

System (19) is stable and has minimum phase transmission zeros. In addition, it has been shown in [Ugalde-Loo, Acha and Licéaga-Castro, 2010] that a stabilizing diagonal controller for this system is given by:

$$\mathbf{K}_{SVC} = \mathrm{diag}\left[\frac{63(s+3.5)(s^2+s+30)}{s^2(s+6)(s+5)}, ... \right.$$
$$\left. \frac{107.5(s+0.43)}{s}, \frac{400}{s} \right] \qquad (21)$$

Calculation of the RGA matrix of system (19) evaluated at $s = 0$ yields

$$\Lambda\big(\mathbf{G}_{SVC}(0)\big) = \begin{bmatrix} 3.43 & -1.88 & -0.55 \\ -2.82 & 5.31 & -1.48 \\ 0.38 & -2.42 & 3.04 \end{bmatrix}, \qquad (22)$$

from where it can be seen that the selected input-output pairings are adequate (according to rule *i* in Section 1). It can be concluded that the compensator has no effect on the steady state coupling.

The input-output pairing can be also investigated using the MSF. In addition, within the ICAD framework it is usual to evaluate the *structural robustness* by measuring the closeness of the Nyquist plot of the MSF to the complex point $(1, 0)$. In short, this allows measuring the robustness of the individual channels to become minimum-phase due to a controller $\mathbf{K}(s)$. A general discussion on this regard can be found in [Leithead and O'Reilly, 1992].

In order to measure *structural robustness*, the Bode plots of the negative of the MSFs are used (*i.e.*, $-\gamma_{ii}(s)$, $i = 1, 2, 3$), which allows classical robustness margins to be considered. These plots are shown in Figure 5, with a perfect control of the remaining variables being assumed. The input-output pairing should be made so that the diagonal MSFs, $\gamma_{ii}(s)$, have the lowest possible gain. Recall that a low coupling at frequency ω_0 is defined as $||\gamma_{ii}(j\omega_0)|| \approx 0$.

For comparison, consider the Bode diagram of $-\gamma_{12}(s)$, which would result if input 1 was paired with output 2. This is shown in Figure 6. The plot suggests that pairing input 1 with output 2 results in Individual Channel 1 being highly coupled with Multi-channel 2-3; thus, this configuration is not recommended. Further examination of the open loop MSFs is omitted in this paper due to space limitations. However, the results are in line with the RGA matrix (22).

Figure 5 shows that although the best input-output pairing selection has been already made, the system lacks structural robustness at low frequencies due to the closeness of the Bode plot to the critical phase and gain values (*i.e.*, 180° and 0 dB), especially in $\gamma_{11}(s)$.

This is where the MSF has advantages over the RGA matrix analysis. For a system to have adequate closed loop robustness the controller must not change the general shape of the Nyquist plot of the diagonal MSFs of the open loop system. The reason is that if the number of encirclements to the point $(1, 0)$ in the Nyquist plot of the MSF changes due to the controller, then the individual channels-zero structure in turn changes and additional non-minimum phase zeros may be induced. In order to assess this fact, the Nyquist plots of the open loop MSFs $\gamma_{ii}(s)$ (with $i = 1, 2, 3$) are shown in Figure 7. The Nyquist diagrams of the corresponding MSFs considering the effects of controller (21) are also shown (these MSFs can be calculated according to equation (10)).

Clearly the effect of controller (21) on the MSFs does not affect the structural robustness (closeness to the point $(1, 0)$). However, the coupling of individual channel 3 with Multi-channel 1-2 has increased. The interpretation of this result must be done carefully, as it does not mean that the closed loop will have increased cross-coupling. Actually, this means that by controlling $y_1(s)$ and $y_2(s)$ through $k_1(s)$ and $k_2(s)$, the re-
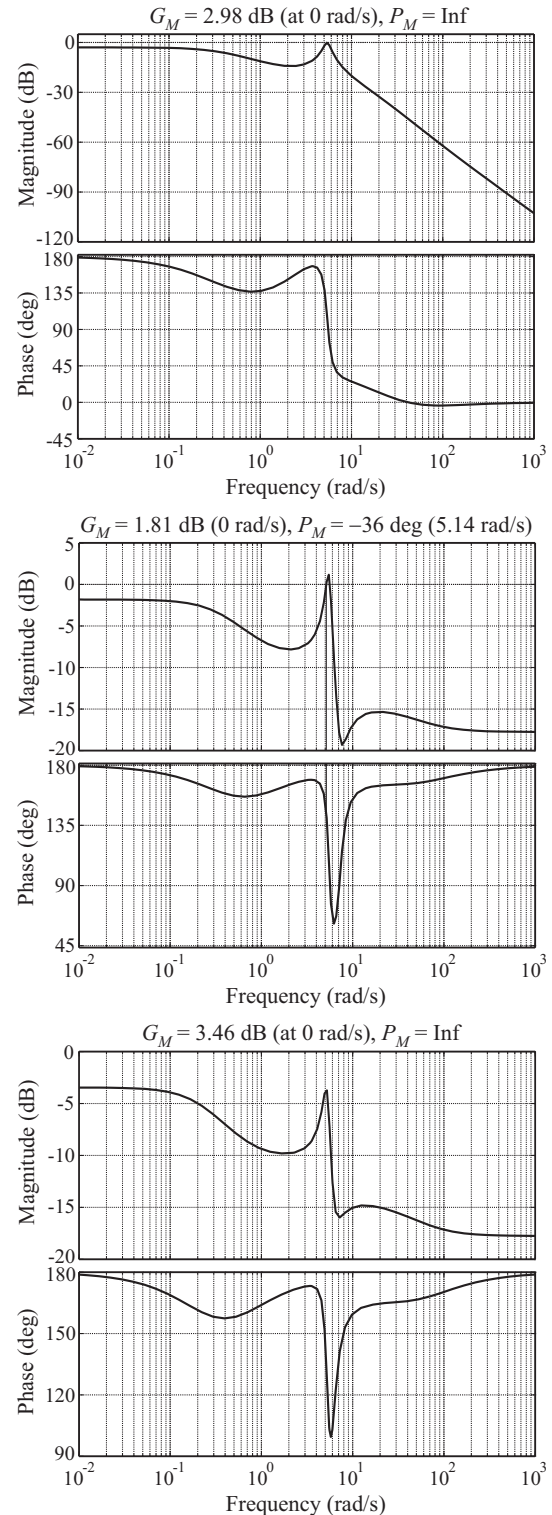

Figure 5.   Bode diagrams of $-\gamma_{ii}(s)$ ($i = 1, 2, 3$).

maining open loop system (*i.e.*, output $y_3(s)$ with input $u_3(s)$) will now be more coupled. However, this coupling can be managed through $k_3(s)$ using the full individual channel transfer function (*i.e.*, considering $k_1(s)$ and $k_2(s)$). On the other hand, the similarity of $\gamma_{11}(s)$ and $\gamma_{22}(s)$ with and without considering the actual controllers allows designing $k_1(s)$ and $k_2(s)$ almost as SISO systems considering the corresponding $\mathbf{H}(s)$ system as an identity (*i.e.*, perfect control on the
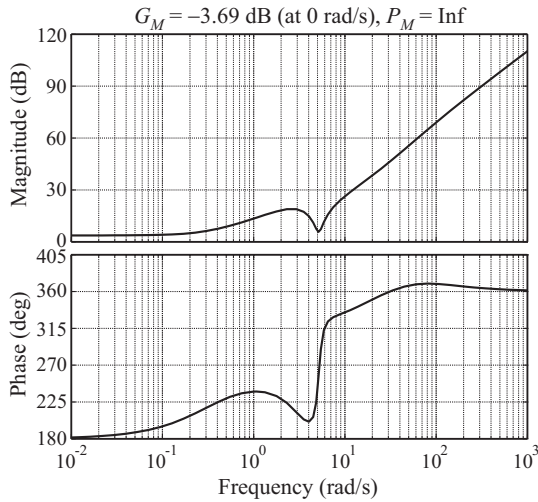
Figure 6.   Bode diagram of $-\gamma_{12}(s)$.

other variables). This clear assessment of robustness and coupling *during* the controller design process cannot be made with the RGA matrix alone.

6   Illustrative Example 2: Four Tanks System

The following example corresponds to a well-known MIMO system which could either be minimum or non-minimum phase. The four tanks system, shown in Figure 8, can be modeled in the frequency domain as follows [Johansson, 2000]:

$$\begin{bmatrix} y_1(s) \\ y_2(s) \end{bmatrix} = \begin{bmatrix} g_{11,tk}(s) & g_{12,tk}(s) \\ g_{21,tk}(s) & g_{22,tk}(s) \end{bmatrix} \begin{bmatrix} v_1(s) \\ v_2(s) \end{bmatrix}, \qquad (23)$$

or, more compactly,

$$\mathbf{Y}_{tk}(s) = \mathbf{G}_{tk}(s)\mathbf{U}_{tk}(s), \qquad (24)$$

with

$$\mathbf{G}_{tk}(s) = \begin{bmatrix} \dfrac{\alpha_1 k_1}{1 + s\tau_1} & \dfrac{(1-\alpha_2)k_1}{(1+s\tau_3)(1+s\tau_1)} \\ \dfrac{(1-\alpha_1)k_2}{(1+s\tau_4)(1+s\tau_2)} & \dfrac{\alpha_2 k_2}{1+s\tau_2} \end{bmatrix}, \qquad (25)$$

where v_1, v_2, are the process inputs (input voltages to the pumps); y_1, y_2, are the outputs (voltages from level measurement devices); k_1, k_2, α_1, α_2, are system constants; τ_i are time constants; and $0 < \alpha_1 < 1$, $0 < \alpha_2 < 1$, and $\tau_i > 0$ with $i = 1, 2, 3, 4$. In particular, α_1 and α_2 model the valves opening percentage. As discussed in [Johansson, 2000; Licéaga-Castro, Navarro-López and Licéaga-Castro, 2008], the system exhibits interacting dynamics since each pump affects both of the outputs. By changing the valve settings, a zero may appear either on the left or the right hand plane.

For this system,

$$\mathbf{G}_{tk}(0) = \begin{bmatrix} \alpha_1 k_1 & (1-\alpha_2)k_1 \\ (1-\alpha_1)k_2 & \alpha_2 k_2 \end{bmatrix}$$
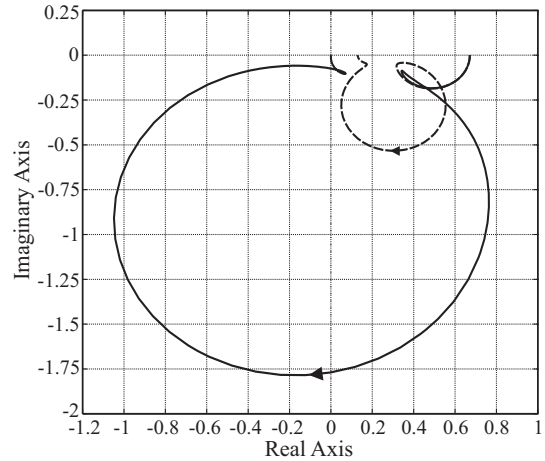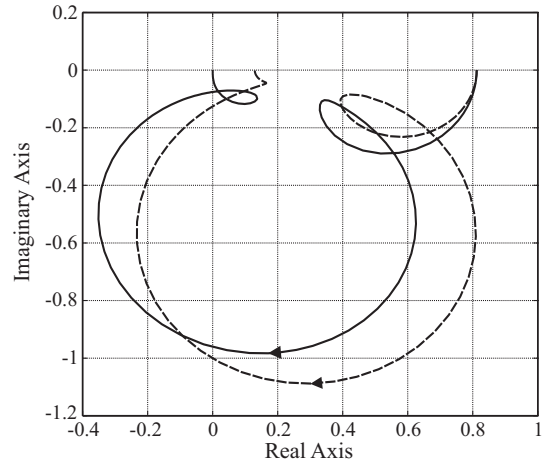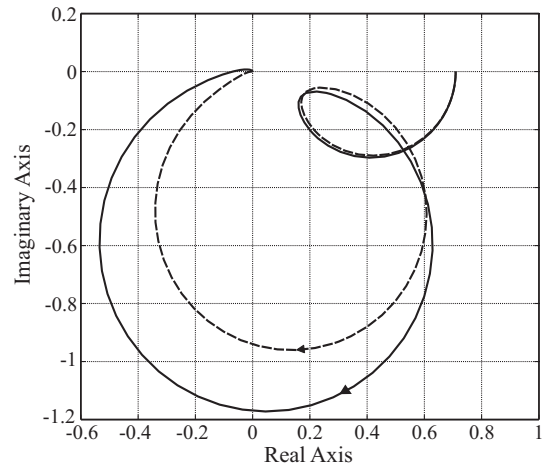
and

Figure 7.   Nyquist plots of open loop (dotted line) and closed loop (continuous) MSFs of $\gamma_{ii}(s)$ $(i = 1, 2, 3)$.

$$\left(\mathbf{G}_{tk}(0)^{-1}\right)^T = \dfrac{\begin{bmatrix} \alpha_1 k_1 & (1-\alpha_2)k_1 \\ (1-\alpha_1)k_2 & \alpha_2 k_2 \end{bmatrix}}{\alpha_1 k_1 \alpha_2 k_2 - (1-\alpha_2)k_1(1-\alpha_1)k_2}$$

Therefore, the RGA matrix of system (25) evaluated at $s = 0$ can be calculated as

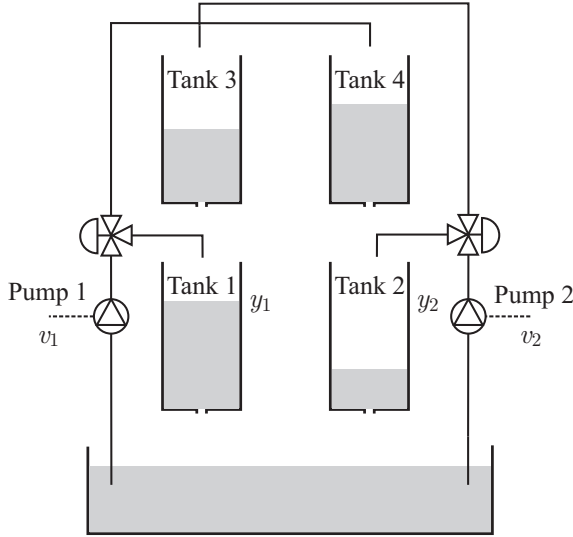$$\mathbf{\Lambda}\left(\mathbf{G}_{tk}(0)\right) = \mathbf{G}_{tk}(0) \times \left(\mathbf{G}_{tk}(0)^{-1}\right)^T,$$

thus,

Figure 8. Schematic diagram of the four tanks system. The water levels in Tanks 1 and 2 are controlled by Pumps 1 and 2.

$$\mathbf{\Lambda}\big(\mathbf{G}_{tk}(0)\big) = \frac{\begin{bmatrix} \alpha_1\alpha_2 & (\alpha_2 - 1)(1 - \alpha_1) \\ (\alpha_2 - 1)(1 - \alpha_1) & \alpha_1\alpha_2 \end{bmatrix}}{\alpha_1 + \alpha_2 - 1} \tag{26}$$

In Section 1 it was discussed that the existence of negative elements on the diagonal of the RGA matrix would imply the loss of integrity (see rule *ii*) [Skogestad and Postlethwaite, 2005]. Recalling that $0 < \alpha_1 < 1$ and $0 < \alpha_2 < 1$ then:

$$\frac{\alpha_1\alpha_2}{\alpha_1 + \alpha_2 - 1} > 0 \Leftrightarrow \alpha_1 + \alpha_2 - 1 > 0. \tag{27}$$

Condition (27) can be used to determine if loss of integrity occurs when controlling the four tanks system. The MSF can also provide this information. Furthermore, it offers additional insight which is useful for the design of adequate controllers. The MSF of system (25) is calculated using (13), yielding:

$$\gamma_{tk}(s) = \frac{(1 - \alpha_1)k_2(1 - \alpha_2)k_1 \prod\limits_{i=1}^{2}(1 + s\tau_i)}{\alpha_1 k_1 \alpha_2 k_2 \prod\limits_{i=1}^{4}(1 + s\tau_i)} \tag{28}$$

$$= \frac{(1 - \alpha_2)(1 - \alpha_1)}{\alpha_1\alpha_2(1 + s\tau_3)(1 + s\tau_4)}.$$

Recall that the individual channels $c_i(s)$ are defined by (17) when the remaining channels are in a closed-loop configuration. In general, for a 2×2 system,

$$c_i(s) = k_{ii}(s)g_{ii}(s)\big(1 - \gamma_{11}(s)h_j(s)\big). \tag{29}$$

with $i, j = 1, 2, i \neq j$, and

$$h_j(s) = \frac{k_{jj}(s)g_{jj}(s)}{1 + k_{jj}(s)g_{jj}(s)}. \tag{30}$$

For clarity, let us rename $\gamma_{11}(s)$ as $\gamma_{tk}(s)$ to put the following explanations in the context of the studied four tanks process. If $\gamma_{tk}(0)h_j(0) > 1$ there will be sign change in the steady state response of the individual channel $c_i(s)$; *i.e.*, sign$\{g_{ii}(0)\} \neq$ sign$\{c_i(0)\}$. This change implies that the closed loop stabilization of $c_i(s)$ in (29) will require destabilization of $g_{ii}(s)$ if integral control is used. This is in fact the definition of loss of integrity. Normally, in an integral control system $h_j(0) \approx 1$ is induced. Therefore, the condition for integrity when integral control is considered can be established in terms of the MSF, defined by (13), as

$$\gamma_{tk}(0) < 1. \tag{31}$$

It can be noticed that the application of condition (31) to MSF $\gamma_{tk}(s)$, given in (28), yields

$$\gamma_{tk}(0) = \frac{(1 - \alpha_2)(1 - \alpha_1)}{\alpha_1\alpha_2} < 1 \Leftrightarrow \alpha_1 + \alpha_2 - 1 > 0. \tag{32}$$

which is similar to the condition established through the RGA matrix in (27).

The minimum phase condition of the transmission zeros of (25) can be also tested with the MSF. In [O'Reilly and Leithead, 1991] it is shown that the following is always true:

$$Z = N + P, \tag{33}$$

where Z is the number of non-minimum phase transfer zeros, P is the number of unstable poles of the MSF and N is the number of clockwise encirclements of the Nyquist plot to the point $(1, 0)$. This is an application of the Nyquist stability criterion. For the four tanks system $P = 0$, *i.e.*, the MSF $\gamma_{tk}(s)$, defined by (28), is always stable. In addition, the relative degree of (28) ensures that

$$\lim_{\omega \to \infty} |\gamma_{tk(j\omega)}| = 0 \text{ and } \lim_{\omega \to \infty} \angle\gamma_{tk(j\omega)} = -180° \tag{34}$$

This implies that there will be a clockwise encirclement of the Nyquist plot to the point $(1, 0)$ *iff* $\gamma_{tk}(0) > 1$; that is, if the Nyquist plot starts to the right of the point $(1, 0)$. Figure 9 shows the Nyquist plot of (28) for different combinations of parameters α_1 and α_2. Notice that when $\alpha_1 = \alpha_2 = 0.35$ or $\alpha_1 = \alpha_2 = 0.4$, the Nyquist plot starts to the right of point $(1, 0)$ and a clockwise encirclement to it occurs, which confirms the previous argument.

Considering the previous discussion, the minimum phase condition for the four tanks system is established by (32), which coincidentally is also the integrity condition. Although the transmission zeros may be obtained through other tools such as the Smith-MacMillan form, the use of ICAD's MSF offers two advantages. Firstly, it allows the assessment of both the integrity and minimum phase conditions, encapsulated in a simple and compact from. Secondly, it permits the
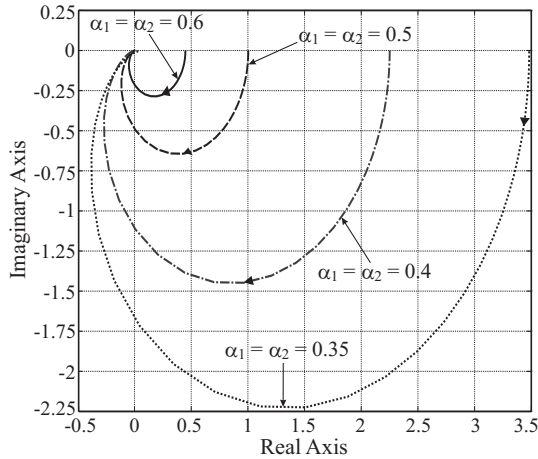
Figure 9.   Nyquist plot of $\gamma_{tk}(s)$ for combinations of α_1 and α_2.

Figure 10.   Nyquist plots of $\gamma_{tk}(s)$, $\gamma_{tk}(s)h_1(s)$ and $\gamma_{tk}(s)h_2(s)$ using diagonal controller (35).

use of any robustness tool based on the Nyquist stability criterion (*e.g., phase and gain margins*, or those available for H$_2$, H$_\infty$, etc.). Thus, the MSF can be used to evaluate the robustness of the transmission zeros. Such assessment is not limited to the open loop analysis, as it is shown next.

Consider the four tanks system (25), with $\alpha_1 = 0.35$, $\alpha_2 = 0.35$, $k_1 = 1$, $k_2 = 2$, $\tau_1 = 1$, $\tau_2 = 1/2$, $\tau_3 = 1/3$ and $\tau_4 = 1/4$. This combination of parameters renders a non-minimum phase condition for the system, as evidence by the Nyquist plot of $\gamma_{tk}(s)$ (see Figure 9). Let a diagonal controller for the four tanks system be defined by

$$\mathbf{K}_{tk} = \text{diag}\big[k_{11}(s), k_{22}(s)\big]$$

$$= \text{diag}\left[\frac{-0.1(s+2)}{s}, \frac{10(s+10)}{s}\right] \quad (35)$$

The effect of non-minimum phase transmission zeros over the actual response of the control system can be better analyzed through the individual channels (29) and the Nyquist stability criterion given by (33). In fact, (33) can be used to test the zeros of $(1 - \gamma_{tk}(s))$; therefore if $h_j(s) = 1$ the zeros of the individual channel $c_i(s)$ (29) will contain the transmission zeros [O'Reilly and Leithead, 1991]. From the definition of $h_j(s)$ in (30), it is clear that the nature of the zeros of the individual channels can be modified through controllers $k_{jj}(s)$. Controllers (35) have been designed so that the zeros of $(1 - \gamma_{tk}(s)h_1(s))$ are minimum phase and the zeros of $(1 - \gamma_{tk}(s)h_2(s))$ are non-minimum phase (for further details on how to achieve this, refer to the procedure given in [Licéaga-Castro, Navarro-López and Licéaga-Castro, 2008]). This allows achieving arbitrarily high bandwidth on individual channel $c_2(s)$ while keeping the effect of the non-minimum phase transmission zeros confined in individual channel $c_1(s)$. These characteristics can be easily confirmed with the Nyquist plots of $\gamma_{tk}(s)h_1(s)$ and $\gamma_{tk}(s)h_2(s)$, shown in Figure 10.

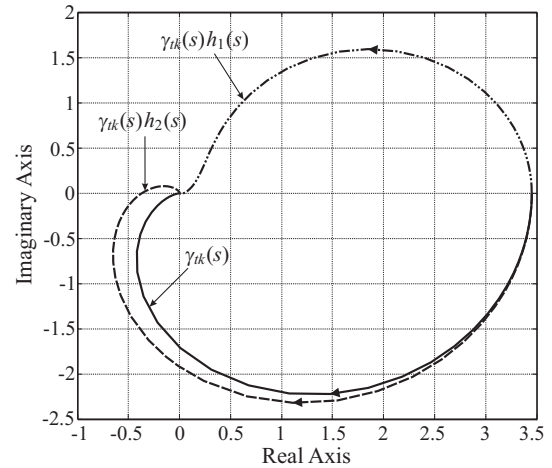Figure 10 shows that $\gamma_{tk}(s)h_2(s)$ preserves the origi-

nal configuration of $\gamma_{tk}(s)$. Therefore, individual channel $c_1(s)$ is non-minimum phase. On the other hand, $\gamma_{tk}(s)h_1(s)$ presents an anti-clockwise encirclement to the point $(1, 0)$, implying that $N = -1$. In addition, note that controller $k_{11}(s)$ has negative gain and an integral action. This will induce one unstable pole in $h_1(s)$ and $P = 1$. This is a necessary condition for integral control since it was determined that the system has no integrity. Thus, according to (33), $Z = 0$, and individual channel $c_2(s)$ is minimum phase.

The insight offered by the analysis of the MSF allows an immediate *robustness* assessment of the individual channels $c_i(s)$ (29) towards the non-minimum phase condition. This can be obtained by measuring the *distance* of the Nyquist plots of $\gamma_{tk}(s)h_1(s)$ and $\gamma_{tk}(s)h_2(s)$ to the point $(1, 0)$. In particular, for this example the gain and phase margins of $\gamma_{tk}(s)h_1(s)$ and $\gamma_{tk}(s)h_2(s)$ result in 11 dB/60° and 11 dB/131°.

The step responses of the control system are shown in Figure 11, which clearly show that system stability has been achieved. Moreover, through the additional information offered by the MSF, it was possible to impose how the non-minimum phase nature of the system affects the final control system design and performance. It can be concluded that the MSF is not only helpful during the design phase of the multivariable controller, but also for the definition of classical robustness measures for the multivariable control system.

7 Conclusion

The results presented in this paper fall short to fully appreciate the use of the ICAD framework. However, the analysis sheds light into the relationship between the MSF and the RGA matrix and allows visualizing how the MSF covers aspects that fall beyond the RGA matrix analysis. This is particularly clear in the control system design process. The MSF can be effectively considered as an alternative to the RGA matrix, allowing to address the effect of specific controllers, the robustness of the system and the evaluation of the cross coupling between groups of input-output pairs.
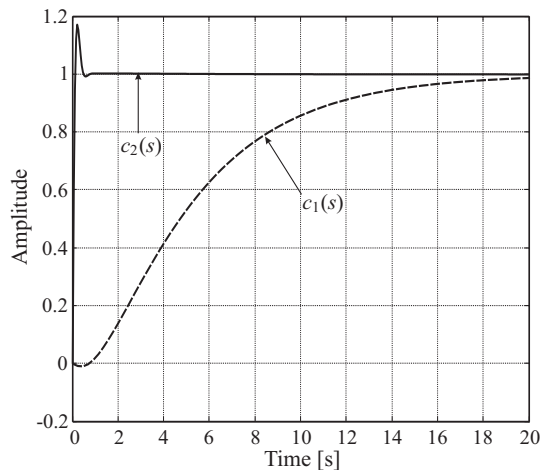
Figure 11. Simulated response of the system outputs to a step reference input.

References

Aree, P., and Acha, E., (1999). *Block diagram model for fundamental studies of a synchronous generator-static VAr compensator system.* IEE Proceedings — Generation, Transmission & Distribution. 146(5), pp. 507–514.

Bristol, E., (1966). *On a new measure of interaction for multivariable process control.* IEEE Transactions on Automatic Control. 11(1), pp. 133–134.

Chiu, M.S., and Arkun, Y., (1990). *Decentralized control structure selection based on integrity considerations.* Industrial & Eng. Chemistry Research. 29(3), pp. 369–373.

Cook, M.V., (2012). *Flight Dynamics Principles: A Linear Systems Approach to Aircraft Stability and Control.* Butterworth-Heinemann, USA.

Grosdidier, P., Morari, M., and Holt, B.R., (1985). *Closed-loop properties from steady-state gain information.* Industrial & Eng. Chemistry Fundamentals. 24(2), pp. 221–235.

Helton, J.W., Stankus, M., and Wavrik, J.J., (1998). *Computer simplification of formulas in linear systems theory.* IEEE Transactions on Automatic Control. 43(3), pp. 302–314.

Johansson, K.H., (2000). *The quadruple-tank process: a multivariable laboratory process with an adjustable zero.* IEEE Transactions on Control Systems Technology. 8(3), pp. 456–465.

Leithead, W.E., and O'Reilly, J., (1992). *M-Input m-output feedback control by individual channel design. Part 1. Structural issues.* International Journal of Control. 56(6), pp. 1347–1397.

Licéaga-Castro, E., Licéaga-Castro, J., and Ugalde-Loo, C.E., (2005). *Beyond the existence of diagonal controllers: from the relative gain array to the multivariable structure function.* In: 44th IEEE Conference on Decision and Control, and European Control Conference (CDC-ECC),

Sevilla, Spain, Dec. 12-15, pp. 7150–7156.

Licéaga-Castro, E., Licéaga-Castro, J., Ugalde-Loo, C.E., and Navarro-López, E.M., (2008). *Efficient multivariable submarine depth-control system design.* Ocean Engineering. 35(17–18), pp. 1747–1758.

Licéaga-Castro, J., Amézquita-Brooks, L., and Licéaga-Castro, E., (2008). *Induction motor current controller for field oriented control using individual channel design.* In: IEEE 34th Annual Conference of Industrial Electronics (IECON), Orlando, USA, Nov. 10-13, pp. 235–240.

Licéaga-Castro, J., Licéaga-Castro, E., and Amézquita-Brooks, L., (2005). *Multivariable gyroscope control by individual channel design.* In: IEEE Conference on Control Applications (CCA), Canada, Aug. 28-31, pp. 785–790.

Licéaga-Castro, E., Navarro-López, E.M., and Licéaga-Castro, J., (2008). *Robust decentralised control design for a MIMO nonminimum-phase process.* In: XIII Congreso Latinoamericano de Control Automatico - VI Congreso Venezolano de Automatizacion y Control, M'erida, Venezuela, Nov. 17-19, pp. 1-6.

Licéaga-Castro, J., Ramírez-España, C., and Licéaga-Castro, E., (2006). *GPC control design for a temperature and humidity prototype using ICD analysis.* In: Computer Aided Control System Design (CACSD), IEEE International Conference on Control Applications (CCA), IEEE International Symposium on Intelligent Control, Oct. 4-6, pp. 978–983.

Mc Avoy, T., Arkun, Y., Chen, R., Robinson, D., and Schnelle, P.D., (2003). *A new approach to defining a dynamic relative gain.* Control Engineering Practice, 11(8), pp. 907–914.

Mithulananthan, N., Canizares, C.A., Reeve, J., and Rogers, G.J., (2003). *Comparison of PSS, SVC, and STATCOM controllers for damping power system oscillations.* IEEE Transactions on Power Systems. 18(2), pp. 786–792.

O'Reilly, J., and Leithead, W.E., (1991). *Multivariable control by 'individual channel design'.* International Journal of Control. 54(1), pp. 1–46.

Skogestad, S., and Postlethwaite, I., (2005). *Multivariable Feedback Control.* John Wiley & Sons, UK.

Ugalde-Loo, C.E., (2009). *Dynamical modelling of power systems with power electronic controllers using individual channel analysis and design.* PhD dissertation, The University of Glasgow.

Ugalde-Loo, C.E., Acha, E., and Licéaga-Castro, E., (2010). *Fundamental analysis of the electromechanical oscillation damping control loop of the static VAr compensator using individual channel analysis and design.* IEEE Transactions on Power Delivery. 25(4), pp. 3053–3069.

Ugalde-Loo, C.E., Acha, E., Licéaga-Castro, E., and Licéaga-Castro, J.U., (2008). *Fundamental analysis of the static VAr compensator performance using individual channel analysis and design.* International Journal of Emerging Electric Power Systems. 9(2), pp. 1–35.